Minimalistic Soft Exosuit for Assisting the Shoulder via Biomechanics-Aware Optimization

Joshi, Sagar; Beck, Irene; Seth, Ajay; Santina, Cosimo Della

DOI
10.1109/Humanoids53995.2022.10000128

Publication date
2022

Document Version
Final published version

Published in
Proceedings of the IEEE-RAS 21st International Conference on Humanoid Robots, Humanoids 2022

2022 IEEE-RAS 21st International Conference on Humanoid Robots (Humanoids)
November 28-30, 2022. Ginowan, Japan.

Minimalistic soft exosuit for assisting the shoulder via biomechanics-aware optimization

Sagar Joshi, Irene Beck, Ajay Seth*, and Cosimo Della Santina*

2022 IEEE-RAS 21st International Conference on Humanoid Robots (Humanoids) | 979-8-3503-0979-9/22/$31.00 ©2022 IEEE | DOI: 10.1109/HUMANOIDS53995.2022.10000128

***Abstract*— Soft exosuits can help to prevent work-related musculoskeletal disorders by offloading human muscles through the application of external forces across the human joints. Many exosuits achieve this through tension producing elements called as exotendons. However, the design of these devices is based on intuition and experience. This leads to potentially sub-optimal or even harmful designs that could cause discomfort or injury to the wearer. This paper deals with automatically finding appropriate attachments and routing locations for exotendons. We propose to do that by accurate musculoskeletal modeling and design parameter optimization of soft exosuits. We focus here on a soft exosuit with a single passive exotendon to assist the shoulder. Using three arm raising-lowering and internal-external rotation motions as examples, we optimize the attachment point and rest-length of the exotendon to reduce overall muscle effort. We then fabricate the exosuit and validate the model predictions by testing with six participants. Supporting the predictions from simulations, measured muscle activity shows reductions in the deltoid and trapezius muscles. This work represents the first instance of explicitly optimizing functional and geometric parameters of exotendons in wearable assistive devices for minimizing human effort.**

I. Introduction

Work-related musculoskeletal disorders are a common occurrence in professions such as assembly lines, farming, and construction. One of the possible ways of addressing this problem is through wearable assistive devices which offload some of the effort taken by the muscles [1]. Rigid exoskeletons [2]–[6] may be unsuited to everyday and widespread usage because they tend to be heavy, bulky, and their movement does not align with biological joints leading to parasitic forces on the skin [7]. In the last decade, there has been a rise in wearable assistive devices made completely using soft materials such as fabric, webbing, artificial tendons, and elastomers [8]–[10]. These devices - known as soft exosuits - are lightweight, conformable, and rely on the wearer's skeleton for structural support.

A large number of these soft exosuits are characterized by harness-like wearable structures that attach to the wearer's body at different locations and actuating elements that pull these structures together [10]. By applying tensile forces externally on the body, these actuating elements or exotendons apply moments across joints thereby reducing the load on biological muscles. Previous studies with such exotendon-driven exosuits have demonstrated their capacity to assist the user in predefined motions of the ankle [11], hip [12], shoulder [13], [14], and elbow [15]–[19]. Despite significant progress, the design of these exosuits, in particular the functional and geometric properties of the exotendons, is based on experience and intuition. For instance, it is not yet understood what should be the optimal attachment or routing location of the exotendons, or what should be their stiffness profile or actuating force. Similarly, it is not how these optimal properties would change for different tasks. An exosuit with sub-optimal exotendon geometry (attachment and routing points) will under-perform and would require possibly larger forces to provide the same level of assistance. This could cause discomfort or possibly injury to the user. Accurate modeling of the human and exosuit could help to address some of these challenges. While some previous studies have used musculoskeletal models for evaluating the performance of assistive devices [20], [21], such modeling has not been applied yet to aid the design phase itself, especially for the upper limb. Furthermore, calculating optimal exotendon properties is additionally challenging for the upper limb due to the complex motion of the shoulder, that includes clavicular and scapular kinematics in addition to the glenohumeral joint [22].

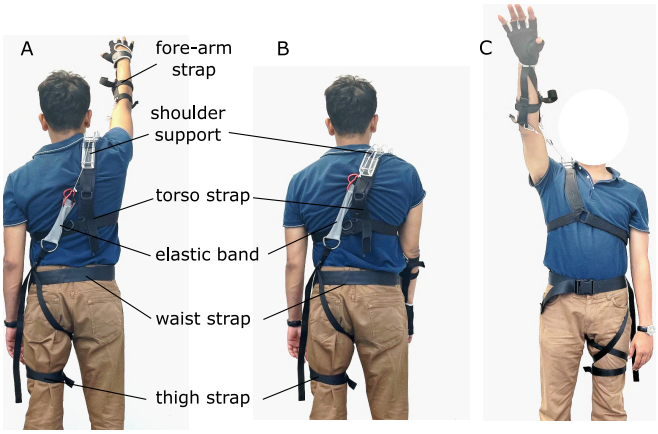

Fig. 1. Prototype of the minimalistic passive soft exosuit for the shoulder that we propose and optimize in this work using a biomechanics-aware strategy. The exosuit interfaces to the wearer at the waist and the arm, connected with an elastic element overlapping the shoulder. (A) Back view, arm flexed. (B) back view, arm extended, (C) front view, arm flexed

The aim of this paper is to address the gap in literature and propose a pipeline for exotendon parameter optimization to minimize wearer's muscle effort. We demonstrate this method for a soft shoulder exosuit consisting of a single passive exotendon. We develop a musculoskeletal model of the human-exosuit system and parameterize its exotendon for functional (rest-length) and geometric (attachment loca-

All authors are with the Mechanical, Maritime, and Materials Engineering Faculty, TU Delft, Delft, The Netherlands. Cosimo Della Santina is also with the Robotics and Mechatronics Department, German Aerospace Center (DLR), Munich, Germany.
* Joint last authors

tion) parameters. We then introduce a biomechanics-aware optimization framework that calculates the muscle effort over a given dynamic motion and looks for the exotendon parameters that minimize this cost function. We demonstrate the proposed method through simulations with three arm raising and internal-external rotation motions. We then validate our approach by prototyping the exosuit and testing with six healthy participants. Experimental results follow the simulations.

To summarize, with this work we contribute to the state of the art of soft exosuits by:

- proposing a pipeline for optimizing functional and geometric parameters of exotendons through a biomechanics-in-the-loop strategy;
- showcasing this idea with extensive simulations;
- designing and implementing a first prototype of the proposed concept;
- testing the prototype with six participants.

II. Baseline Design of the Exosuit

In multi-body systems, it has been found that appropriately shaping the elastic fields around joints could be used to reduce energy and power requirements [23], [24]. Therefore, we argue that a completely passive device has the potential to offset the loads taken by the biological joints of the body. Furthermore, as the functionality is pre-programmed mechanically into the device, it does not require additional control methods.

We focus on assisting the shoulder joint because muscles acting at this joint are affected the most during elevated and overhead tasks [1]. For this first study, we adopt a minimalistic approach and define the baseline design for our shoulder exosuit as shown in Fig. 1, consisting of a single passive exotendon attached at the arm and waist, and overlapping the shoulder. As the arm moves, the passive exotendon will store and release energy at the shoulder joint, thereby assisting the wearer. For improved wearability and performance, we include two design considerations: (i) use of low-friction elements on the shoulder to support the exotendon, and (ii) extending the attachments on the arm and waist to larger regions on the body to distribute the exotendon forces, reduce shear on skin, and increase stiffness of the exosuit-human interface.

Even with such a minimalistic approach, the forces applied by the exosuit on the wearer are governed by several design parameters, both functional (stiffness and rest-length), and geometric (attachment locations, routing locations, moment arm over shoulder). Here, we focus on two design parameters: rest-length and attachment point at the waist. We fix its other parameters, namely - stiffness, arm attachment location, and wrapping over the shoulder.

III. Human and Exosuit Model

We propose here a human-exosuit musculoskeletal model as depicted in Fig. 2. We use the open-source biomechanical platform OpenSim [25], [26] to implement, visualize, simulate and analyze this model.

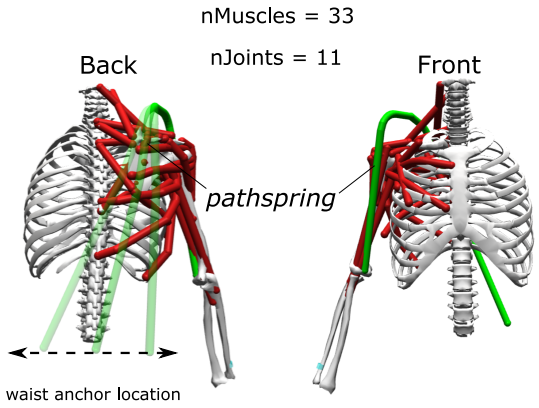

Fig. 2. Proposed biomechanical model including the musculoskeletal model (with 33 muscles in red and 11 joints) and the exotendon attached at the forearm and waist. We show both back and front view. We use the former to show the effect of varying the waist attachment location.

The human model is based on the thoraco-scapular musculoskeletal model defined in [22], [27]. This model is characterized by (i) eleven degrees of freedom of the right arm - three rotations for the glenohumeral joint, two rotations for the clavicle with respect to the thorax, four rotations for the scapula gliding over the thorax, and one each for elbow extension-flexion, and elbow pronation-supination, (ii) a point constraint on the scapula and clavicle, representing the acromion joint, and (iii) thirty-three Millard-type musculotendon actuators [28] representing the muscles of the upper torso and arm. The forces applied by the muscles are a function of the activation values and are governed by the maximum isometric value F_{max}, and characteristic curves defining the force-stretch, force-velocity, and passive force-stretch properties. The muscle forces create moments across joints, which drive the motion. During a dynamic task, the muscle activation values evolve over time in order to support the inertial and external moments on the joints at each instant.

To model the exosuit, we need to consider the exotendon interaction forces. An exotendon applies tension forces at its points of attachment and reaction forces at regions where it overlaps the wearer's body. In our exosuit, the exotendon is attached at the arm and waist, and overlaps the shoulder. We neglect friction at the shoulder overlap as we use low-friction elements (details in Section V) and assume equal tension at the two attachment points. To model this exotendon we use a *pathspring* object (included in the standard OpenSim library), which is defined by its path constraints and mechanical properties. It applies only tension force linearly proportional to its stiffness (K) and extension as follows: $F_s = K \times (\texttt{extendedLength} - \texttt{restLength})$. The path constraints of the *pathspring* are defined by two sets: *PathPointSet* and *PathWrapSet*. The *pathspring* is constrained to pass through the points defined in the *PathPointSet*, and to wrap around surfaces defined in the *PathWrapSet*. When stretched, the *pathspring* applies tension forces at its end points, and reaction forces at the intermediate points and surfaces defined in the *PathPointSet* and *PathWrapSet* respec-

tively. These reaction forces are calculated in OpenSim based on change in direction of the *pathspring* at the corresponding intermediate points and surfaces.

In our human model, we anchor the *pathspring* on the humerus at the elbow joint center (between medial and lateral epicondyles), and at the waist at an adjustable point on the line connecting the left and right PSIS (posterior edges of the iliac crest). Additionally, we constrain the *pathspring* to (i) overlap the upper back, modeled using a wrapping ellipsoid on the torso and (ii) pass over a shoulder support bracket, modeled using one path point and two wrapping cylinders, placed on the right clavicle. The final routing path of the *pathspring* is: waist path point - upper torso wrapping ellipsoid - shoulder wrapping cylinder 1 - shoulder path point - shoulder wrapping cylinder 2 - humerus path point. The resulting model is shown Fig. 2. We set its stiffness to 500 N/m, equal to the elastic resistance band (Kaytan Latex resistance band - light) that we use later in our prototype. As stated in Section II, the *rest length* and location of the waist attachment point represent the functional and geometric parameters respectively for our exotendon design optimization.

IV. Exotendon Optimization

This section introduces the biomechanics-aware optimization, which relies on the model introduced in Sec. III.

A. Defining the objective function

In order to optimize the exotendon design parameters, we need a reliable method to quantify its effect on the wearer. To this end, we propose a metric to represent the cumulative muscle effort required to perform a given task:

$$f(X) = \int_{t_0}^{t_f} \sum_{i=1}^{N_\mathrm{m}} (a_i(X,t))^2 dt, \tag{1}$$

where X is a vector holding the exotendon design parameters of rest-length and waist attachment point, $0 < a_i(X,t) < 1$ is the activation of the i-th muscle fascicle at time t, N_m is the total number of muscle fascicles, and t_0 and t_f are the initial and final times, respectively.

The muscle activations are determined by the neuromuscular system of our body so as to produce the desired motion at the joints. Thus, for finding the optimal exosuit configuration, we first need to reliably predict the muscle activations. As there are more number of muscles, 33, than degrees of freedom, 11, this problem becomes non-trivial.

B. Solving muscle redundancy

The neuromuscular system uses the muscles efficiently so as to minimize overall effort or energy [29] while producing the desired motion. We simulate this functionality using static optimization [29]. We first calculate the desired velocities and accelerations by filtering and differentiating the joint kinematics data of the motion being considered. Then we use built-in functions in OpenSim that calculate the joint

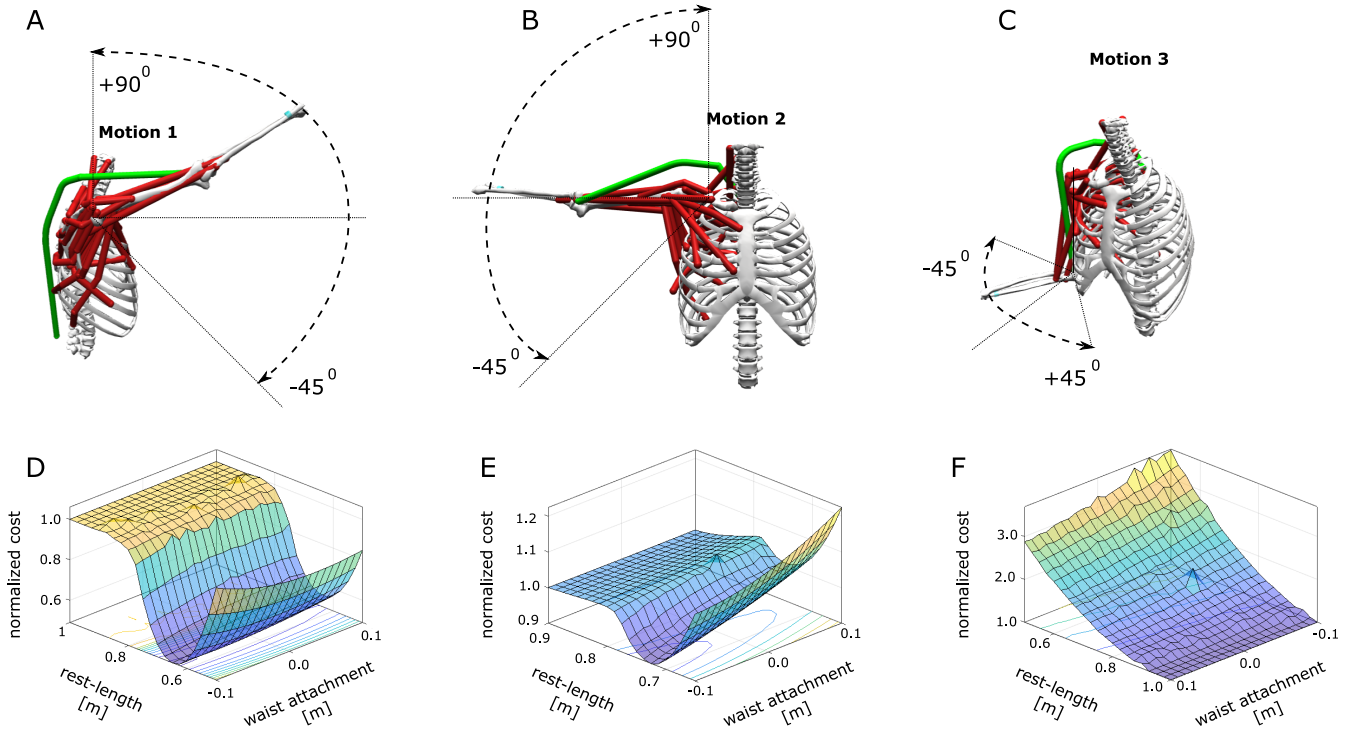

Fig. 3. Selected motions for the study shown via the musculoskeletal model, and evolution of (1) when varying the two design parameters. Evaluating the cost entails solving the muscle redundancy problem (2) at each time step and summing for the entire motion. We report the results for three different motions: (A) Selected motion 1: Flexion-extension of the shoulder from -45^0 to $+90^0$ and back. (B) Selected motion 2: Abduction-adduction of the shoulder from -45^0 to $+90^0$ and back. (C) Selected motion 3: Internal-external rotation of the shoulder from -45^0 to $+45^0$ and back. (D) Normalized cost surface for motion 1, (E) Normalized cost surface for motion 2, (F) Normalized cost surface for motion 3.

accelerations generated by the muscles as a function of their activation values. Finally, we define a cost function as the norm of muscle activations. The static optimization problem for solving the muscle redundancy problem is then formulated as:

$$\begin{aligned} \min_{a_i} \quad & \sum_{i=1}^{N_\mathrm{m}} (a_i)^2 \\ \text{s.t.} \quad & \ddot{q}_j^d = \ddot{q}_j([a]) \\ & 0 \leq a_i \leq 1 \end{aligned} \tag{2}$$

where $\ddot{q}_j^d$ is the desired acceleration at the j^{th} joint, and $\ddot{q}_j([a])$ is the acceleration generated by the set of muscle activations $[a]$ at the j^{th} joint. The above quantities are defined for a single time step, and the muscle activations for dynamic motions are calculated by conducting the above static optimization for each time step.

C. Considered motions

We consider three motions of the shoulder for this study:

1) flexion-extension from -45^0 to the horizontal, to 90^0 and back to -45^0, as shown in Fig. 3A
2) abduction-adduction from -45^0 to the horizontal, to 90^0 and back to -45^0, as shown in Fig. 3B , and
3) internal-external rotation from -45^0 to the forward axis to 45^0, and back as shown in Fig. 3C

D. Simulation study

We simulated different configurations for the exotendon in its parameter space and calculated the cumulative muscle effort required to perform the three motions above using (1). We defined a grid of 21x21 values for the rest-length - between 0.4 and 1 m; and waist attachment point - between -0.1 m (left side) +0.1 m (right side). While changing the attachment location also changes the exotendon pretension, this effect is negligible as compared to the range of considered exotendon rest-lengths. We simulated each condition for the three considered motions. Fig. 3D-F show the cost surfaces for different exotendon configurations while performing the three considered motions. The cost surfaces have been normalized with the no exosuit condition such that a value of 1 corresponds to a cumulative muscle effort without an exosuit. The flat regions on all three cost surfaces with value of 1 correspond to the conditions when the exotendon has a large rest-length making it slack for the entire motion, and therefore applying no force on the human.

We see that for motions 1 and 2, the exosuit reduces muscle effort in some configurations, but could also increase the effort if the rest-length is too short. This is because for these shorter rest-lengths, the body has to act against the spring, requiring more effort. We also see that for motions 1 and 2, the optimal location of the waist attachment is -0.1m, which corresponds to the side of the body opposite of the supported arm. Lastly, we see that for the optimal exosuit configuration, the muscle effort is significantly reduced for motion 1, close to 50% of no-exosuit condition. For motion 2, the best exosuit configuration reduces effort by only 10% than the no exosuit case. This suggests that the exosuit baseline design is well-suited for motion 1, but should be improved for motion 2. This can be done by changing some of the fixed parameters such as stiffness, and allowable attachment locations.

For motion 3, we see that there is an increase in the muscle effort while using the exosuit in all simulation conditions. This suggests that the baseline exosuit design presented is not suitable to support this motion, and therefore needs to be modified, either by changing the attachment regions completely, or the stiffness of the exotendon. These simulation results help to identify the optimal exotendon attachment points and thus aid in customizing exosuit design to the desired motion. This methodology also helps to filter out baseline designs for the given motion without requiring expensive fabrication and testing cycles.

Lastly, we see small spikes on the cost surface for all three motion. This can be attributed to the presence of the acromion joint constraint between the clavicle and scapula motions, which must be considered when finding the joint

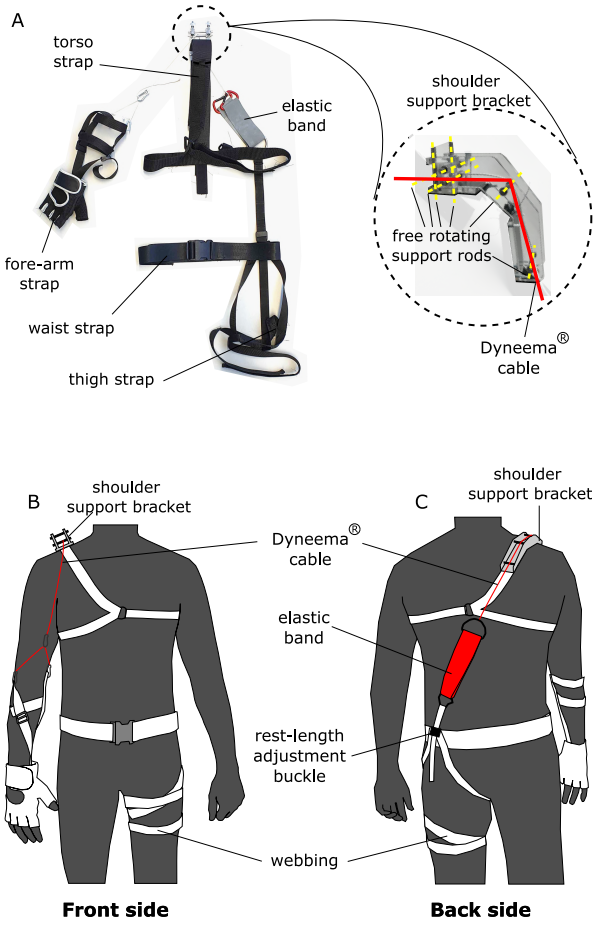

Fig. 4. Prototype of the minimalistic passive soft exosuit for the shoulder. It interfaces to the wearer at the waist and the arm, and overlaps the shoulder over free rotating rods on a support bracket. Additional attachments at the fore-arm and thigh help to safely transmit forces to the user by applying predominantly normal forces on the skin. (A) The fabricated prototype. (B) Schematic of the exosuit showing the front side. (C) Schematic of the exosuit showing the back side.

velocities and accelerations during static optimization. We will address this in future studies.

V. Exosuit Design and Fabrication

For the exosuit design, we focused on assisting motion 1 and chose the optimized parameters of attachment location and rest-length using the simulation results from Fig. 3D. The main considerations for the exosuit design were: (i) device should be lightweight, (ii) anchor locations should be at load-bearing locations with suitable padding wherever necessary, (iii) interaction forces should act normally on the skin, (iv) exosuit size should be easy to adjust for different participants, (v) friction should low on the shoulder to allow free motion of the exotendon. Based on these, we fabricated the exosuit as shown in Fig. 4.

The exosuit is primarily made using nylon webbing and the various sections are fastened on the wearer via length-adjustable buckles and Velcro® fasteners. The exotendon itself is made using an elastic resistance band (Kaytan Latex resistance band, stiffness = 500N/m). It is affixed at the arm webbing with an inextensible Dyneeema® rope (2mm diameter) and at the waist with a webbing strap. The exotendon rest-length was defined as the length between the arm and waist attachments when the elastic band just begins to stretch. A length-adjustment buckle at the waist allows to easily change the exotendon rest-length. To minimize shear forces on the arm, we extend the webbing straps over the forearm and transfer the exotendon forces to the hand using a glove. Similarly, at the waist, the exosuit consists of a waist belt reinforced with additional webbing straps that transfer the exotendon forces to the thigh. The arm and waist webbing straps are adjusted carefully while donning the exosuit so that the exotendon does not apply any moment on the elbow and hip joints. A rigid bracket placed on the right shoulder supports the exotendon as it wraps over the shoulder. This shoulder support bracket, as shown in Fig. 4A, is made using laser-cut parts of 6mm thick acrylic sheet, and houses six freely rotating steel rods to support and redirect the exotendon with minimal friction. By having two horizontal and two vertical rods at the front-side, this attachment can support the exotendon when the arm is flexing to the front or the side. Lastly, to safely distribute the loads from the exosuit to the user, the inner side of the entire exosuit is padded with 4mm thick ethylene copolymer foam. The fabricated exosuit weighs 600 grams.

VI. Experimental Validation

A. Testing conditions

We tested the exosuit with six male participants (H:1.78± 0.06m; W: 72 ± 6.8kg) and measured their muscle activity while performing motion 1. The participants were recruited after informing them of the experiment, and signing a consent form. The study was approved by the Human Research Ethics Committee of Delft University of Technology. After donning the exosuit, we calculated the optimal exotendon rest-length for each participant scaled according to their height, and set this value using the length adjustment buckle at the waist. The participants were then asked to flex and extend the arm ten times, while following a video of the OpenSim model performing motion 1. During the test, we measured the surface electromyography (EMG) activity of four muscles - deltoid anterior, mid, and posterior, and trapezius scapula - using Delsys® surface EMG sensors (inter-electrode distance of 20mm). The sensors were placed as shown in Fig. 5A after preparation according to Cram [30]. The test was repeated under two conditions: with and without exosuit.

After data collection, we processed the raw EMG by first high pass filtering at 100 Hz, followed by full-wave rectification, and then low-pass filtering at 4 Hz, according to [31]. The processed EMG data was normalized by maximum voluntary contractions measured at the end of the experiment.

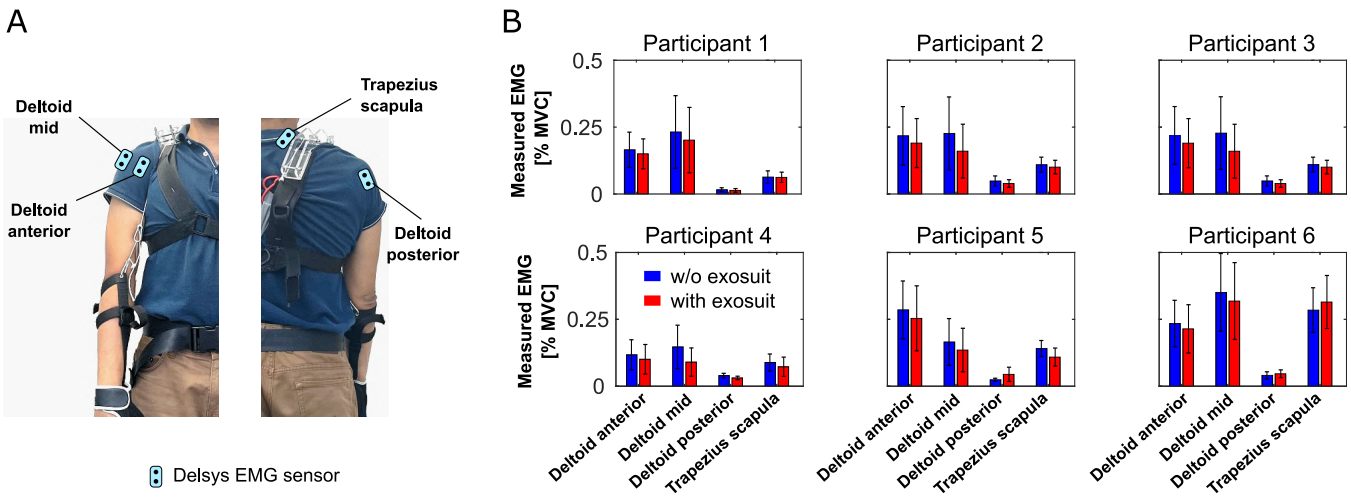

Fig. 5. Experimental testing with the exosuit: (A) Placement of the surface EMG sensors, (B) Bar plots showing root-mean-squared values and standard deviations of activation values of four muscles of the six participants while performing Motion 1. In all figures, blue and red bars represent no exosuit and exosuit condition respectively.

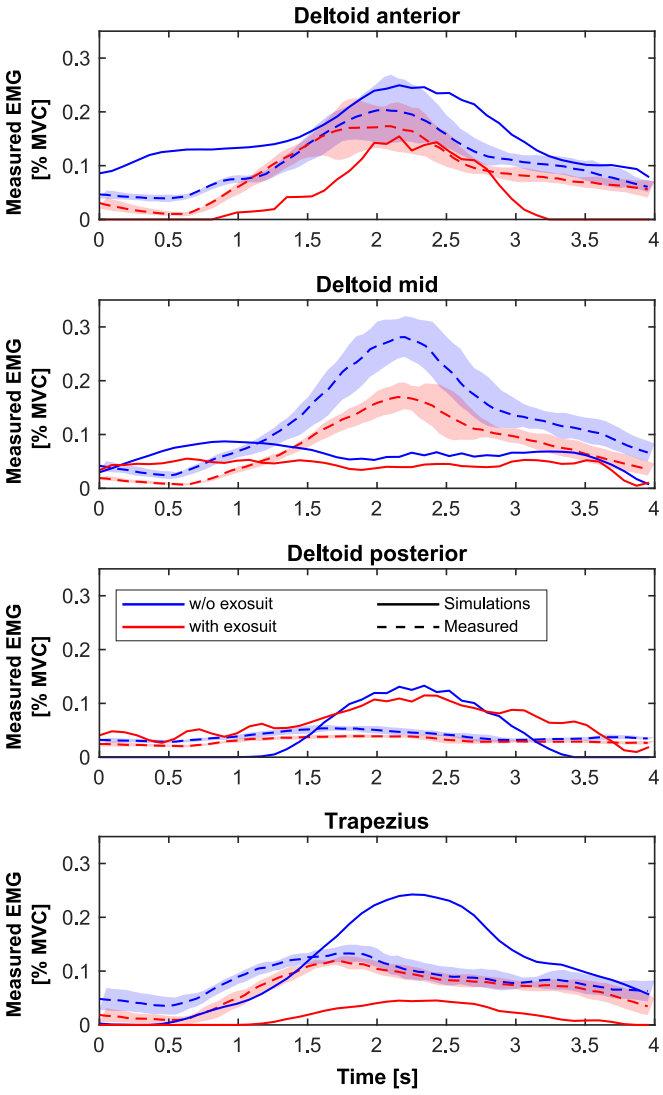

Fig. 6. Simulated vs. measured muscle activation of participant 4 while performing motion 1. The continuous and dotted curves correspond to simulated and measured values respectively. Similarly, the blue and red curves represent no exosuit condition and exosuit condition respectively. The shaded regions show the standard deviation for each corresponding condition.

B. Results

Fig. 5B shows the root-mean-squared (RMS) and standard deviations of the measured EMG activity of the six participants under the two conditions. We can see that the use of the exosuit reduced muscle activity of almost all the measured muscles for all participants. This reaffirms the fact that the exotendon is able to share the load taken by the muscles while performing the task. At the same time, we see an increase in activity of the deltoid posterior for participants 5 and 6. As this muscle is the primary shoulder extensor, an increase in its activity while using the exosuit suggests that for participants 5 and 6, the rest-length was too small and the participants had to counteract the exotendon forces in order to extend the arm back. Furthermore, participant 6 also shows an increase in trapezius muscle activity. As the exosuit forces try to depress the clavicle and scapula, the trapezius has to act to lift and support the shoulder. This will be addressed in future studies by scaling the model appropriately for each participant and then finding the participant-specific optimal exotendon configuration.

Fig. 6 shows the evolution of muscle activity of Subject 4 while performing the flexion-extension task. The continuous curves correspond to simulated values and the dotted curves correspond to the RMS measured values, averaged over the ten cycles. The shaded regions show the corresponding standard deviation at each time step. We can see that there is some correlation between the simulations and measured values of the deltoid anterior muscle. But for the remaining three muscles, the simulations and measured muscle activity show slightly different patterns. This can be attributed to the difference in joint kinematics of the simulations and experiments. The simulated motion, taken directly from an older study [27], consists of pure flexion-extension with the arm pointing in the forward axis. During testing, however, the motion was a combination of flexion-extension and abduction-adduction, to prevent the exotendon from contacting the EMG sensors. This explains the much higher measured muscle activity in the deltoid mid muscle, which acts during shoulder abduction. In future studies, we will address this by measuring the actual motion of each participant and conducting participant-specific simulations.

VII. Conclusions

Exotendons in previous exosuits are designed by intuition and experience, and therefore are prone to sub-optimal or possibly even harmful designs. In this paper, we demonstrated optimization of functional and geometric parameters of an exotendon for the first time with a passive shoulder exosuit as an example. Using this approach, it is now possible to iterate through different exotendon configurations and optimize or reject baseline exosuit designs without expensive and time-consuming trial-and-error methods. The presented pipeline can be easily extended to more parameters of the exotendon, such as the stiffness and force profiles, as well as locations over the shoulder, arm, and torso. Looking further ahead, it could be used for systems with several exotendons assisting other joints of the body, as well as for optimizing control of active exotendons. While results were mostly positive, there were some limitations of this study which will be addressed in future work.

Our motion for the simulations did not exactly match that of the participants, which is the primary reason for deviation between simulation and measured muscle activity. Similarly, we adjusted the exotendon for each participant by scaling exotendon rest-length to their respective heights. In future studies, we will address these issues by measuring the actual motion of each participant and scaling musculoskeletal models for participant-specific simulations. Despite these limitations, the exosuit was still able to reduce the measured muscle activity for all six participants, suggesting some robustness to uncertainties. This aspect will be studied in more detail in future studies to ensure that the optimal configuration for one motion does not negatively impact

another one. By enabling a biomechanics-aware exotendon optimization strategy, this work represents an important step towards reducing the stress during manual material labor.

ACKNOWLEDGMENTS

The authors would like to thank Tim Verburg, for assisting in fabrication.

REFERENCES

[1] Tjaša Kermavnar, Aijse W de Vries, Michiel P de Looze, and Leonard W O'Sullivan. Effects of industrial back-support exoskeletons on body loading and user experience: an updated systematic review. *Ergonomics*, 64(6):685–711, 2021.

[2] Joshua Hull, Ranger Turner, Athulya A Simon, and Alan T Asbeck. A novel method and exoskeletons for whole-arm gravity compensation. *Ieee Access*, 8:143144–143159, 2020.

[3] Hazreen H Harith, Muhammad Fuad Mohd, and Sharence Nai Sowat. A preliminary investigation on upper limb exoskeleton assistance for simulated agricultural tasks. *Applied Ergonomics*, 95:103455, 2021.

[4] Logan Van Engelhoven and Homayoon Kazerooni. Design and intended use of a passive actuation strategy for a shoulder supporting exoskeleton. In *2019 Wearable Robotics Association Conference (WearRAcon)*, pages 7–12. IEEE, 2019.

[5] Aijse Willem de Vries, Frank Krause, and Michiel Pieter de Looze. The effectivity of a passive arm support exoskeleton in reducing muscle activation and perceived exertion during plastering activities. *Ergonomics*, 64(6):712–721, 2021.

[6] Marco Rossini, Sander De Bock, Arthur van der Have, Louis Flynn, David Rodriguez-Cianca, Kevin De Pauw, Dirk Lefeber, Joost Geeroms, and Carlos Rodriguez-Guerrero. Design and evaluation of a passive cable-driven occupational shoulder exoskeleton. *IEEE Transactions on Medical Robotics and Bionics*, 3(4):1020–1031, 2021.

[7] José L Pons. *Wearable robots: biomechatronic exoskeletons*. John Wiley & Sons, 2008.

[8] Michael Wehner, Brendan Quinlivan, Patrick M Aubin, Ernesto Martinez-Villalpando, Michael Baumann, Leia Stirling, Kenneth Holt, Robert Wood, and Conor Walsh. A lightweight soft exosuit for gait assistance. In *Robotics and Automation (ICRA), 2013 IEEE International Conference on*, pages 3362–3369. IEEE, 2013.

[9] Alan T Asbeck, Robert J Dyer, Arnar F Larusson, and Conor J Walsh. Biologically-inspired soft exosuit. In *2013 IEEE 13th International Conference on Rehabilitation Robotics (ICORR)*, pages 1–8. IEEE, 2013.

[10] Michele Xiloyannis, Ryan Alicea, Anna-Maria Georgarakis, Florian L Haufe, Peter Wolf, Lorenzo Masia, and Robert Riener. Soft robotic suits: State of the art, core technologies, and open challenges. *IEEE Transactions on Robotics*, 2021.

[11] Alan T Asbeck, Stefano MM De Rossi, Kenneth G Holt, and Conor J Walsh. A biologically inspired soft exosuit for walking assistance. *The International Journal of Robotics Research*, 34(6):744–762, 2015.

[12] Alan T Asbeck, Kai Schmidt, and Conor J Walsh. Soft exosuit for hip assistance. *Robotics and Autonomous Systems*, 73:102–110, 2015.

[13] Anna-Maria Georgarakis, Jaeyong Song, Peter Wolf, Robert Riener, and Michele Xiloyannis. Control for gravity compensation in tendon-driven upper limb exosuits. In *2020 8th IEEE RAS/EMBS International Conference for Biomedical Robotics and Biomechatronics (BioRob)*, pages 340–345. IEEE, 2020.

[14] Anna-Maria Georgarakis, Michele Xiloyannis, Peter Wolf, and Robert Riener. A textile exomuscle that assists the shoulder during functional movements for everyday life. *Nature Machine Intelligence*, pages 1–9, 2022.

[15] Leonardo Cappello, Dinh Khanh Binh, Shih-Cheng Yen, and Lorenzo Masia. Design and preliminary characterization of a soft wearable exoskeleton for upper limb. In *2016 6th IEEE International Conference on Biomedical Robotics and Biomechatronics (BioRob)*, pages 623–630. IEEE, 2016.

[16] Domenico Chiaradia, Michele Xiloyannis, Chris W Antuvan, Antonio Frisoli, and Lorenzo Masia. Design and embedded control of a soft elbow exosuit. In *2018 IEEE International Conference on Soft Robotics (RoboSoft)*, pages 565–571. IEEE, 2018.

[17] Nicola Lotti, Michele Xiloyannis, Guillaume Durandau, Elisa Galofaro, Vittorio Sanguineti, Lorenzo Masia, and Massimo Sartori. Adaptive model-based myoelectric control for a soft wearable arm exosuit: A new generation of wearable robot control. *IEEE Robotics & Automation Magazine*, 27(1):43–53, 2020.

[18] Michele Xiloyannis, Leonardo Cappello, Khanh D Binh, Chris W Antuvan, and Lorenzo Masia. Preliminary design and control of a soft exosuit for assisting elbow movements and hand grasping in activities of daily living. *Journal of rehabilitation and assistive technologies engineering*, 4:2055668316680315, 2017.

[19] Michele Xiloyannis, Domenico Chiaradia, Antonio Frisoli, and Lorenzo Masia. Physiological and kinematic effects of a soft exosuit on arm movements. *Journal of neuroengineering and rehabilitation*, 16(1):1–15, 2019.

[20] Xianlian Zhou and Liying Zheng. Model-based comparison of passive and active assistance designs in an occupational upper limb exoskeleton for overhead lifting. *IISE Transactions on Occupational Ergonomics and Human Factors*, pages 1–19, 2021.

[21] Sagar Joshi and Abhishek Gupta. Conceptual design of an active transtibial prosthesis based on expected joint and muscle forces in a unilateral transtibial amputee: A modelling study. In *ASME 2015 International Mechanical Engineering Congress and Exposition*, pages V003T03A042–V003T03A042. American Society of Mechanical Engineers, 2015.

[22] Ajay Seth, Ricardo Matias, António P Veloso, and Scott L Delp. A biomechanical model of the scapulothoracic joint to accurately capture scapular kinematics during shoulder movements. *PloS one*, 11(1):e0141028, 2016.

[23] Cosimo Della Santina and Alin Albu-Schaeffer. Exciting efficient oscillations in nonlinear mechanical systems through eigenmanifold stabilization. *IEEE Control Systems Letters*, 5(6):1916–1921, 2020.

[24] Luigi Bono Bonacchi, Máximo A Roa, Anna Sesselmann, Florian Loeffl, Alin Albu-Schäffer, and Cosimo Della Santina. Efficient and goal-directed oscillations in articulated soft robots: the point-to-point case. *IEEE Robotics and Automation Letters*, 6(2):2555–2562, 2021.

[25] Scott L Delp, Frank C Anderson, Allison S Arnold, Peter Loan, Ayman Habib, Chand T John, Eran Guendelman, and Darryl G Thelen. Opensim: open-source software to create and analyze dynamic simulations of movement. *IEEE transactions on biomedical engineering*, 54(11):1940–1950, 2007.

[26] Ajay Seth, Jennifer L Hicks, Thomas K Uchida, Ayman Habib, Christopher L Dembia, James J Dunne, Carmichael F Ong, Matthew S DeMers, Apoorva Rajagopal, Matthew Millard, et al. Opensim: Simulating musculoskeletal dynamics and neuromuscular control to study human and animal movement. *PLoS computational biology*, 14(7):e1006223, 2018.

[27] Ajay Seth, Meilin Dong, Ricardo Matias, and Scott Delp. Muscle contributions to upper-extremity movement and work from a musculoskeletal model of the human shoulder. *Frontiers in neurorobotics*, page 90, 2019.

[28] Matthew Millard, Thomas Uchida, Ajay Seth, and Scott L Delp. Flexing computational muscle: modeling and simulation of musculotendon dynamics. *Journal of biomechanical engineering*, 135(2), 2013.

[29] Frank C Anderson and Marcus G Pandy. Static and dynamic optimization solutions for gait are practically equivalent. *Journal of biomechanics*, 34(2):153–161, 2001.

[30] Eleanor Criswell. *Cram's introduction to surface electromyography*. Jones & Bartlett Publishers, 2010.

[31] Hermie J Hermens, Bart Freriks, Roberto Merletti, Dick Stegeman, Joleen Blok, Günter Rau, Cathy Disselhorst-Klug, and Göran Hägg. European recommendations for surface electromyography. *Roessingh research and development*, 8(2):13–54, 1999.